

Earthquake stress triggers, stress shadows, and seismic hazard

Ruth A. Harris

US Geological Survey, Mail Stop 977, 345 Middlefield Road, Menlo Park, CA 94025, USA

Many aspects of earthquake mechanics remain an enigma at the beginning of the twenty-first century. One potential bright spot is the realization that simple calculations of stress changes may explain some earthquake interactions, just as previous and ongoing studies of stress changes have begun to explain human-induced seismicity. This paper, which is an update of Harris¹, reviews many published works and presents a compilation of quantitative earthquake-interaction studies from a stress change perspective. This synthesis supplies some clues about certain aspects of earthquake mechanics. It also demonstrates that much work remains to be done before we have a complete story of how earthquakes work.

Introduction

LARGE earthquakes nucleate, propagate, and terminate. That much we do know. But what about the physics of why, when, and where these actions occur? The complete picture of earthquake-mechanics remains unresolved. To help solve at least part of the complex puzzle sooner rather than later, I have focused here on the role of stress changes in earthquake mechanics. In this paper I tackle the topics of earthquake promotion, or triggering, and earthquake delay, or deferment, due to earthquake-generated changes in stress. Among the questions that I attempt to answer: Can we understand and adequately model the mechanics of local inter-earthquake and intra-earthquake triggering and prevention? Do earthquake-induced static or dynamic stress changes trigger subsequent earthquakes? Is there a triggering threshold? Can stress shadow (regions where faults are relaxed) calculations be used to estimate where and when future earthquakes will not occur? With this paper I delve into some earthquake-interaction topics that have drawn special attention. I primarily concentrate on research that has performed quantitative estimates of earthquake-generated stress changes and applied these calculations to the study of earthquake interactions. For a review of earthquake triggering by man-made and other natural mechanisms, the reader is referred to McGarr and Simpson².

e-mail: harris@jog.wr.usgs.gov

Background

Although human-induced earthquakes, through activities such as fluid injection and withdrawal, mining, and hydrocarbon recovery have been recognized for decades^{2,3} the impact of interactions between natural earthquakes has not been as well understood. Pioneering papers⁴⁻⁹ presented calculations of mainshock static stress changes affecting subsequent earthquake locations, but these preliminary determinations were not formally adopted by the scientific community for use in earthquake hazard assessment. Part of the reason may have been that the static stress changes discussed were thought to be small, of the order of 0.1 MPa (1 bar), a value that is just a fraction of the stress-drop during an earthquake. Also, the original results were predominantly qualitative in nature and hard to judge quantitatively. In the subsequent 15 to 20 years, a large body of additional research has been added to the original work.

There is now an internationally-distributed data set of static stress changes, generated by large earthquakes, influencing the timing and location of subsequent 'natural' earthquakes⁴⁻⁶⁸. Many of the authors have used calculations of a Coulomb stress increment (Figure 1) calculated from an elastic-dislocation model of the mainshock⁶⁹⁻⁷¹ and have examined the geographical pattern of subsequent earthquakes relative to the pattern of change in Coulomb failure stress. Almost all of these studies profess finding a positive correlation between the number (or rate) of aftershocks, or the occurrence of subsequent mainshocks, and regions of calculated stress increase. Many of the studies also show a deficiency (or rate decrease) of aftershocks, or subsequent mainshocks, in regions of calculated stress decrease.

Landers earthquake

Perhaps the most publicized calculations of static stress changes were made following the 1992 *M* 7.3 Landers earthquake in southern California^{24,25,27}. This large earthquake occurred near the populous San Bernardino region of the San Andreas fault. Soon after the earthquake's location and mechanism were determined, it became apparent that the estimated static stress effect of the Landers earthquake was to reduce the normal stress on

part of the San Andreas fault. Calculations made shortly after the Landers earthquake estimated that Landers had hastened the next large earthquake on the San Andreas fault by about 1 to 2 decades^{24,25,27}, if its nucleation point were to fall in the area of reduced normal stress. Unfortunately the timing of the next large San Andreas fault earthquake could not be assigned an absolute value since no one knew precisely when the next San Andreas earthquake was due to occur, or where it might nucleate, even without the normal stress change. In the meantime, after-slip along the Banning fault, that lies in close proximity to the San Andreas, has been inferred⁷², and the San Andreas fault has, as of December 1999, not yet slipped in the next large or great earthquake.

I now address a range of failure criteria that have been used to model earthquake interactions, both in the vicinity of the Landers earthquake and elsewhere. I start with the simplest model, Coulomb failure stress, then explore more complex hypotheses. Table 1 provides a snapshot of some of the theories by very briefly describing the required parameters, mentioning a few of the successes and failures, and listing some related papers.

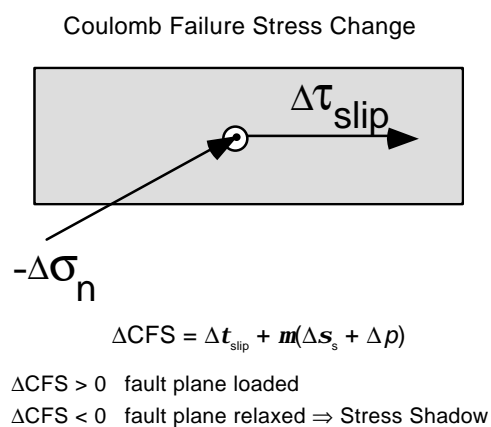


Figure 1. ΔCFS , the change in Coulomb failure stress, or Coulomb stress increment, is used to evaluate if one earthquake brought another earthquake closer to, or farther from, failure. If $\Delta CFS > 0$, the first earthquake brought the second earthquake closer to failure; if $\Delta CFS < 0$, the first event sent the second event farther away from failure, and into a stress shadow. The stress shadow lasts for the length of time that it takes the second fault plane to recover from the stress increment. One manner of recovery is through long-term tectonic loading. ΔCFS is resolved onto the fault plane and in the slip direction of the second earthquake, at the hypocentre of the second earthquake; Δt_{slip} is the change in shear stress due to the first earthquake resolved in the slip direction of the second earthquake. $\Delta \sigma_n$ is the change in normal stress due to the first earthquake, resolved in the direction orthogonal to the second fault plane. $\Delta \sigma_n > 0$ implies increased tension; m is the coefficient of friction and Δp is the change in pore pressure. Many recent authors have simplified this equation by dropping the explicit calculation of Δp and using an apparent coefficient of friction, m' . The simplified equation (eq. (4)) and assumptions behind m' are discussed in the text.

Coulomb failure stress

Spatial patterns of static stress changes calculated using Coulomb-failure assumptions⁷³ (Figure 1) seem to correlate well with spatial patterns of aftershocks; more aftershocks commonly occur where the change in Coulomb stress is positive than where the change is negative. With Coulomb failure, earthquakes that occur in regions of increased Coulomb static stress are said to have been advanced towards failure by the positive stress increment. From a simple elastic perspective, the amount of advance, Δt , equals $\Delta CFS/\dot{\epsilon}$ where ΔCFS is the change in Coulomb failure stress (Figure 1), and $\dot{\epsilon}$ is the long-term stressing rate. Examples of inferred advancement (where the subsequent earthquake(s) have already occurred) are the cascade of earthquakes this century on the North Anatolian fault in Turkey^{51,56,68} and the 1954 Rainbow Mountain–Fairview Peak–Dixie Valley, Nevada earthquakes³⁹.

Stress shadows

Similarly, Coulomb stress change theory has been successfully applied to situations where faults were relaxed, the result of a negative change in Coulomb failure stress, $\Delta CFS < 0$. For cases where a fault is relaxed or put into a stress-shadow³⁸, one can calculate the time that it should take for long-term tectonic loading to recover the static stress change. The time change, now a delay, is simply expressed as $\Delta CFS/\dot{\epsilon}$ and is the time required to bring the fault back to its state of stress before it was relaxed.

ΔCFS time-delay calculations were performed by Simpson *et al.*¹⁷, after it was noted that creepmeters along the right-lateral San Andreas fault moved left-laterally following the nearby 1983 magnitude 6.7 Coalinga earthquake in central California¹¹. Simpson *et al.*¹⁷ estimated that the 1983 Coalinga earthquake delayed the next moderate Parkfield earthquake on the San Andreas fault in central California by at least one year. This technique of using Coulomb stress changes to estimate time-delays has also been applied to larger earthquakes. Simpson and Reasenber³², Jaumé and Sykes⁴², and Harris and Simpson⁵⁴ calculated the effects of the great 1906 San Francisco earthquake on nearby active faults. The 1906 earthquake, which ruptured the San Andreas fault in central and northern California, relaxed many of the San Francisco Bay area faults and delayed subsequent large earthquakes for decades. Simpson and Reasenber³² determined that after 1906, large earthquakes on nearby faults disappeared, then later reappeared at a time consistent with models of long-term tectonic reloading. Simpson and Reasenber also made estimates of the effects of the large 1989 Loma Prieta earthquake on nearby San Francisco Bay area faults. Lienkaemper *et al.*⁷⁴ validated these estimates by calculating that the resumption of creep on

the Hayward fault is consistent with tectonic erosion of the 1989 stress shadow. We now examine the intricacies of the ΔCFS calculations by going back to ‘first principles’, then explore the range of parameters used in such calculations.

Coulomb stress change defined

Using Coulomb failure assumptions⁷³, one can define a Coulomb failure stress, CFS such that

$$\text{CFS} = |\bar{\boldsymbol{t}}| + \boldsymbol{m}(\boldsymbol{s} + p) - S, \tag{1}$$

where $|\bar{\boldsymbol{t}}|$ is the magnitude of the shear traction on a plane, \boldsymbol{s} is the normal traction (positive for tension) on the plane, p is the fluid pressure, S is the cohesion, and \boldsymbol{m} is the coefficient of friction. If one assumes that \boldsymbol{m} and S are constant over time, then a change in CFS is

$$\Delta\text{CFS} = \Delta|\bar{\boldsymbol{t}}| + \boldsymbol{m}(\Delta\boldsymbol{s} + \Delta p). \tag{2}$$

Note that the first term on the right side of eq. (2) implies an isotropic failure plane – a more realistic assumption might require the plane to always fail by slipping in a constant rake direction, in which case the first term becomes $\Delta\boldsymbol{t}_{\text{rake}}$ or $\Delta\boldsymbol{t}_{\text{slip}}$ (Figure 1), which is the change in shear stress in the rake direction. The advantage of using

changes in stress is that often, absolute values of stress are not known, but stress change values can be calculated fairly readily from information about the geometry and slip direction of an earthquake rupture. (The exact details of geometry and slip also become less important the farther one goes from the rupture.) If a preferred rake direction and a fault plane orientation are known for a fault that has experienced a stress change, then $\Delta\boldsymbol{t}_{\text{rake}}$ can be calculated directly from the stress change tensor. If the fault plane is assumed to be isotropic, then calculation of $\Delta|\bar{\boldsymbol{t}}|$ requires some knowledge of the pre-existing ‘regional’ stress field, although simplifying assumptions can be made^{15,30}.

In order to approximate the effects of pore pressure changes on the change in CFS, one needs to make some assumptions. One possible end-member assumption is that the medium is homogeneous and isotropic. Then, for the undrained situation immediately after the static stress changes have occurred, but before fluids have had a chance to flow freely, Rice and Cleary⁷⁵ and Roeloffs^{76,77} have shown that

$$\Delta p = -\boldsymbol{b}' \Delta \boldsymbol{s}_{\text{kk}} / 3, \tag{3}$$

where \boldsymbol{b}' for rock is similar to Skempton’s⁷⁸ coefficient \boldsymbol{b} that was determined for soils and depends on the bulk moduli of the material and the fraction of volume that the fluid occupies⁷⁵; $\boldsymbol{s}_{\text{kk}}$ is the sum of the diagonal elements

Table 1. Summary of stress change approaches

Method	Parameters required	Successes	Problems
Static Coulomb failure stress (Elastic) ΔCFS	Mainshock static slip-model, \boldsymbol{m}' , and $\Delta\boldsymbol{s}$, $\Delta\boldsymbol{t}$, $\bar{\boldsymbol{t}}$, on known fault planes and known slip-directions*.	$\Delta\text{CFS} > 0$ explains locations of aftershocks that do occur. $\Delta\text{CFS} < 0$ predicts shadows (timing and locations). May give rupture extent.	Many $\Delta\text{CFS} > 0$ faults do not experience subsequent large earthquakes, so it is hard to use $\Delta\text{CFS} > 0$ as a predictive tool. Does not predict size of impending aftershock. Does not explain delayed failure.
Dynamic Coulomb failure stress (Elastic) $\Delta\text{CFS}(t)$	Mainshock dynamic fault slip-model, \boldsymbol{m}' , and $\Delta\boldsymbol{s}(t)$, $\Delta\boldsymbol{t}(t)$ on known fault planes and known slip-directions*.	May predict rupture lengths, given fault geometry.	Does not explain long delays (> tens of seconds) between subevents. Needs more testing.
Static rate-and-state	Mainshock static slip-model, $\Delta\boldsymbol{s}$, $\Delta\boldsymbol{t}$, \boldsymbol{s} , \boldsymbol{t} , $\bar{\boldsymbol{t}}$, A , B , D_c , H , time of last event, recurrence interval (to determine slip speed).	Seems to predict aftershock duration.	Needs more testing. Rate-and-state parameters defined in the lab, but not known for the earth.
Dynamic rate-and-state	Mainshock dynamic fault slip-model, $\Delta\boldsymbol{s}(t)$, $\Delta\boldsymbol{t}(t)$, \boldsymbol{s} , \boldsymbol{t} , $\bar{\boldsymbol{t}}$, A , H , time of last event, slip speed.	May explain remote triggering.	Needs more testing. Still need to define rate-and-state parameters in the earth. Inertial terms not yet included in models.
Static Coulomb failure stress (Viscoelastic)	Mainshock slip-model, Maxwell relaxation time, relaxing layer thickness.	May explain time delays between mainshock and subsequent events, also irregular recurrence intervals.	Needs more testing, also needs more geodetic data to confirm viscoelastic parameters.
Fluid flow	Mainshock slip model, permeability tensor.	May explain time delays between mainshock and subsequent events.	May not be successful at predicting both the spatial and temporal aftershock patterns.

*If the aftershock fault planes are not known, then some authors assume optimally oriented faults; this requires knowledge of the background stress directions.

of the stress tensor. From Skempton⁷⁸, \mathbf{b} theoretically ranges from 0 (dry soil) to 1 (fully saturated soil). \mathbf{b}' has been measured to range from 0.47 (Indiana limestone at 30 MPa external stress⁷⁹), to approximately 1.0, with values of 0.7 to 1.0 often reported^{80,81}. (Wang⁸² has reported laboratory observations suggesting terms in addition to those appearing in eq. (3) may be needed.)

A more-complex assumption is that the fault zone materials are more ductile than the surrounding materials, as in the model of Rice⁸³, so that $\mathbf{s}_{xx} = \mathbf{s}_{yy} = \mathbf{s}_{zz}$ in the fault zone, and therefore $\Delta\mathbf{s}_{kk}/3 = \Delta\mathbf{s}$. In this case, with the assumptions that the medium is homogeneous and isotropic outside of the fault zone and that the medium is homogeneous and isotropic inside of the more-ductile fault zone, one can obtain

$$\Delta\text{CFS} = \Delta|\bar{\mathbf{f}}| + \mathbf{m}'\Delta\mathbf{s}, \quad (4)$$

where $\mathbf{m}' = \mathbf{m}(1 - \mathbf{b}')$.

It has become common in the literature to state the CFS change (eq. (4)) without detailing the assumptions regarding pore fluid behaviour. The parameter \mathbf{m}' is often called the apparent coefficient of friction and is intended to include the effects of pore fluids as well as the material properties of the fault zone. This strategy is mostly an attempt to cover up our lack of knowledge about the role of pore fluids. Strictly speaking, although a constant \mathbf{m}' can account for instantaneous pore fluid behaviour, in some cases⁸³, this may not be true in general. Comparing eq. (4) with eqs (2) and (3), for example, it is noted that for the homogeneous isotropic poroelastic model, \mathbf{m}' is a function of $\Delta\mathbf{s}_{kk}$ and $\Delta\mathbf{s}$:

$$\mathbf{m}' = \mathbf{m} \left(1 - \frac{\mathbf{b}'}{3} \frac{\Delta\mathbf{s}_{kk}}{\Delta\mathbf{s}} \right). \quad (5)$$

Although it is convenient to lump our ignorance of pore fluid behaviour into a redefined 'apparent coefficient of friction', \mathbf{m}' , we run the risk of missing some important clues in interpreting our data. Beeler *et al.*⁸⁴ have deprecated the use of \mathbf{m}' in favour of explicit use of \mathbf{m} and Δp for this reason and the interested reader is referred to that paper for a thorough discussion of the friction coefficient. Nonetheless, in the discussion that follows, we will use \mathbf{m}' in the non-rigorous way that has become commonplace.

A study of the stress changes produced by earthquakes in the Harvard catalog⁸⁵ and earthquakes from the combined Harvard, Preliminary Determination of Epicenters (PDE), and California Institute of Technology/US Geological Survey (CIT/USGS) southern California catalogues⁸⁶ suggest $\mathbf{m}' = 0$. Reasenberg and Simpson²⁶ showed that $\mathbf{m}' = 0.2$ best fit the Loma Prieta aftershock data and, Gross and Bürgmann⁸⁷ who used a different technique to estimate \mathbf{m}' also found low values most appropriate. A range of \mathbf{m}' , between 0 and 0.6, is preferred by Deng and Sykes⁴⁷. These numbers are for different time-periods,

and for different tectonic settings. The Reasenberg and Simpson²⁶ study covered a few years of Loma Prieta aftershocks in the San Francisco Bay area of California, whereas Deng and Sykes⁴⁷ covered a decade of small earthquakes in southern California. Parsons *et al.*⁶⁴ proposed that different faults may be described with different values of \mathbf{m}' . They analysed the pattern of seismicity following the 1989 Loma Prieta, California, earthquake and inferred a higher value of \mathbf{m}' for the San Francisco Bay area minor oblique (right-lateral thrust) faults, and a lower value for the major strike-slip faults such as the San Andreas fault. Some have proposed that \mathbf{m}' in the CFS equations may actually change with time, due to migrating pore fluids²⁴⁻²⁶.

Fluid flow

The migrating pore fluid and changing pore pressure hypothesis explain the physics behind some human-induced seismicity²⁻³. This hypothesis has also been used to explain inter-earthquake relations. Nur and Booker⁸⁸ suggested that mainshock-induced pore pressure changes may control the timing of aftershocks. Similarly, Li *et al.*¹⁴ attempted to observe a spatial and temporal shift in aftershock locations due to pore fluid flow, and Hudnut *et al.*¹⁸ used pore pressure changes to explain an 11-hour delay between two adjacent earthquakes in 1987 that occurred on conjugate fault planes in southern California. Jaumé and Sykes²⁵ discussed the potential effects of pore fluid flow in the aftermath of the 1992 Landers earthquake, but the implications have not yet been tested. The study by Noir *et al.*⁸⁹ of an earthquake sequence in Central Afar also supports the fluid flow hypothesis. On the opposite side, some workers have proposed that fluid-flow cannot be the sole explanation for aftershock triggering, since aftershocks appear to predominantly occur at the edges of mainshock high-slip regions⁹⁰. Scholz⁹¹ also argued that aftershocks would not be occurring simultaneously over the entire mainshock rupture plane if fluid flow alone were responsible.

Coulomb stress change magnitude threshold

It appears that static stress changes as low as 0.01 MPa (0.1 bar) can affect the locations of aftershocks^{26,30,53,92}. This value is just a fraction of the stress drop during earthquakes, which is one reason that Coulomb stress changes are said to 'enhance' or 'encourage' the occurrence of an earthquake, as opposed to generating the earthquake (but also see Gomberg *et al.*⁹³ for another viewpoint). Can static stress change smaller than 0.01 MPa (0.1 bar) also trigger, or delay earthquakes? This remains an unresolved issue. In some instances smaller stress changes do appear correlated with patterns of seismicity

occurrence^{38,47,56}, but there are often not enough events to allow a rigorous statistical test. One exception is the thorough quantitative study by Anderson and Johnson⁹² who examined the 1987 Superstition Hills, California earthquake sequence. They found no evidence for stress triggering of the aftershocks except when the mainshock-induced stress changes exceeded 0.1 to 0.3 bars or the aftershocks occurred from 1.4 to 2.8 years after the mainshocks.

Coulomb stress changes: Static near-field studies

Although the majority of Coulomb failure models assume that the location of interest is far away from the first earthquake so that one can ignore fine details of its slip distribution (this distance is quantified by Hardebeck *et al.*⁵³ for the Landers and Northridge earthquakes), a few papers have ambitiously tackled the near-field topic^{45,48,66,94–98}. Caskey and Wesnousky⁴⁵, Nostro *et al.*⁴⁸, and Perfettini *et al.*⁶⁶ suggest that the static stress changes induced by the faults or earthquakes that ruptured first may have influenced the amounts of slip on the subsequently-ruptured faults. On a similar note, Crider and Pollard⁹⁸, who examined fault interaction in the near-field, concentrated on the generic case of interacting normal faults. They used geologic field observations and numerical modelling to determine how, where, and if individual normal faults may grow and link up to become more complex structures. Their findings may assist in the development of ‘cascade’ models for normal faulting earthquakes, i.e. determining how large a normal fault earthquake can become. The Crider and Pollard results may also prescribe when and where to expect sizable normal faulting aftershocks.

In a study of the specific case of low-angle normal faults, Axen⁹⁹ found that although the record of mainshocks on these shallowly dipping faults may be sparse, earthquakes do occur on these faults and damaging subevents (and subsequent main events) on the low-angle faults can also be triggered by slip on steeper-dipping normal faults. He cites examples from earthquakes in Nevada, Italy, and Turkey. Axen’s⁹⁹ interpretations include the effects of pore pressure changes.

Taylor *et al.*⁵⁹ modelled Δ CFS generated by three great subduction earthquakes. They examined whether Δ CFS was consistent with the position, timing, and, in contrast to other studies, the mechanisms of aftershocks in the upper plate for each of the great earthquakes. For the most part, Δ CFS appears to have been a plausible explanation for the simplified case of mainshock slip isolated on a single asperity.

Aseismic slip models

In opposition to many of the CFS studies discussed in the paper, some near-field studies of earthquakes have come

to different conclusions than their far-field counterparts. Both Beroza and Zoback⁹⁴ and Kilb *et al.*⁹⁷ examined the near-field static stress effect of the 1989 M_w 6.9 Loma Prieta mainshock on its nearby aftershocks. Beroza and Zoback⁹⁴ concluded that the calculated (near-field) mainshock static stress changes did not do a better than random job at determining the aftershock mechanisms. One possibility they proposed was that dynamic strains or pore pressure changes influenced the locations of aftershocks. Kilb *et al.*⁹⁷ examined a similar data set, with the addition of an assumed homogeneous background stress field to the calculated stress changes. Kilb *et al.* concluded that it was possible to use a static stress change model and simulate the observed aftershock mechanism diversity, but only if the initial stress level in the crust was quite low, lower than would be required to have generated the Loma Prieta mainshock. Therefore, Kilb *et al.* also concluded that some other factors must explain the aftershock pattern. Their considered options included dynamic stresses, pore pressure changes, an inhomogeneous background stress field, the driving stresses of aseismic deep-slip, and also the possibility that the initial assumptions of fault geometry were not accurate.

In a study of the Upland earthquake sequence (1988–1990) in southern California, Astiz *et al.*¹⁰⁰ showed that calculated Coulomb stress changes generated by the moderate earthquakes do not match the aftershock pattern. Whereas the aftershocks primarily occur on one side of the fault plane, the Coulomb stress pattern for optimally-oriented faults predicts symmetry. Similarly Hardebeck *et al.*⁵³ had difficulty matching the pattern of aftershocks following the 1994 Northridge, California earthquakes with the Coulomb stress pattern inferred for the mainshock.

Dodge *et al.*^{95,96} have also suggested that static stress-triggering increments in the near-field do not explain all earthquake interactions. In a departure from the usual studies of large earthquakes triggering smaller ones, Dodge *et al.*^{95,96} looked at the relationship between initial smaller events and the subsequent larger earthquake in a sequence. Dodge *et al.*⁹⁵ examined foreshocks of the 1992 Landers, California earthquake and found that the largest foreshocks probably did not trigger the beginning (an M_w 4.4 subevent) of the Landers mainshock. Their calculations showed predominantly zero or negative cumulative CFS at the site of the M_w 4.4 subevent as a result of the occurrence of the largest foreshocks. They used this result to conclude that fault-zone geometry, rather than static stress-triggering increments, controlled where the Landers mainshock nucleated, and that the entire Landers foreshock sequence may have been driven by aseismic creep (also see Deng and Sykes⁴⁶ for a different viewpoint). That aseismic creep controls the rupture process is the key idea of earthquake instability models¹⁰¹. Dodge *et al.*⁹⁶ extended their previous work by looking at five more foreshock–mainshock sequences in California in addition

to Landers and found that four out of six (including Landers) of the foreshock–mainshock sequences did not follow a simple Coulomb failure (static) stress change model of earthquake triggering.

Perfettini *et al.*⁶⁶ arrived at the same result as Dodge *et al.*⁹⁶ for the relationship between the moderate-magnitude foreshocks of 1988 and 1989 and the 1989 Loma Prieta, California mainshock; the foreshocks do not appear to have pushed the mainshock hypocentre towards failure. To step out of this conundrum, Perfettini *et al.*⁶⁶ observed that the maximum mainshock slip did occur in the region of increased foreshock stress change. Therefore Perfettini *et al.* proposed that the foreshocks did influence the mainshock rupture process although the connection between the foreshocks and mainshock hypocentre did not follow traditional expectations.

Rate-and-state friction

Laboratory-derived constitutive equations have also been applied to the study of earthquake interactions. One such set of equations is termed ‘rate-and-state’, because in the laboratory observations that the equations describe, fault strength is dependent on slip-rate and on slip and time history of the fault. Rate-and-state equations allow for a time delay before the onset of failure. They also describe how some faults may slide stably, whereas others experience ‘stick-slip’ motion. A number of authors have derived or considered rate-and-state friction models (e.g. see Scholz¹⁰² for a review), but for this article, I summarize the results of only two papers: Dieterich¹⁰³ and Dieterich and Kilgore¹⁰⁴ who have made simple testable predictions of the effects of stress changes on aftershock timing and locations using rate-and-state equations.

Whereas Coulomb friction invokes the simple eq. (1) to describe the failure limit, rate-and-state formulations use a more complex relation which also describes the evolution of quantities as they approach failure. For example, a simplified, one state-variable form of rate-and-state friction is¹⁰⁴:

$$t = s \left[m_0 + A \ln \left(\frac{\dot{d}}{\dot{d}^*} \right) + B \ln \left(\frac{q}{q^*} \right) \right], \quad (6)$$

where \dot{d} is the sliding speed, q is a state-variable that can be interpreted to represent the effects of contact time between the two surfaces of a fault, and m_0 , A and B are empirically determined coefficients. $A - B > 0$ leads to stable sliding; $B - A > 0$ leads to instability (stick-slip behaviour). The asterisked terms are normalizing constants.

In the rate-and-state formalism, an earthquake nucleates on a fault when the sliding speed, \dot{d} ‘runs away’ and increases dramatically above interseismic values (to speeds

of the order of centimetres per second). Dieterich¹⁰³ [eq. (A13)] gives the time-to-failure in terms of the sliding speed and other variables:

$$t = \frac{As}{\dot{t}} \ln \left(1 + \frac{\dot{t}}{Hs\dot{d}} \right), \quad (7)$$

where

$$H = \frac{-k}{s} + \frac{B}{D_c}, \quad (8)$$

t is the time-to-failure, \dot{t} is the long-term stressing rate, k is the effective stiffness for source nucleation, B is a fault constitutive parameter, and D_c is the characteristic sliding distance (see Table 2 for more definitions).

If an external factor, such as a static stress change generated by a nearby earthquake, perturbs the sliding speed, it also changes the eventual nucleation time or time-to-

Table 2. Definitions

t	Shear stress
t_0	Initial shear stress before an external stress step
Δt	Shear stress change
Δt_{slip}	Shear stress change resolved in the slip-direction
s, s_n	Normal stress*
s_0	Initial normal stress before an external stress step*
$\Delta s, \Delta s_n$	Normal stress change*
S	Cohesion
\dot{t}	Tectonic loading rate
CFS	Coulomb failure stress
ΔCFS	Change in Coulomb failure stress
Δt	Change in time-to-failure due to a change in stress
b	Skempton’s coefficient for soils
b'	Skempton-like coefficient for rock
p	Pore pressure
Δp	Change in pore pressure
m	Coefficient of friction
m'	Apparent coefficient of friction
m_0	Empirically determined rate-and-state coefficient
t	Time-to-failure
D_c	Critical slip distance (m)
k	Spring stiffness
H	A combination of rate-and-state parameters (eq (8))
B	An empirically determined rate-and-state coefficient
A	An empirically determined rate-and-state coefficient
a	An empirically determined rate-and-state parameter
q	State variable
q^*	A normalizing constant
\dot{d}	Slip speed
\dot{d}_0	Initial slip speed before an external stress step
\dot{d}^*	A normalizing constant

*The Coulomb failure and rate-and-state equations use different sign conventions for the normal stress. In the CFS equations negative s indicates compression, whereas in the rate-and-state equations of Dieterich¹⁰³, for example, positive s indicates compression.

failure. Following Dieterich¹⁰³, during the long interval of self-driven accelerating slip and before an externally applied stress change, a fault's sliding speed depends on the initial stress and state. After a stress-step occurs, the slip speed depends on the new stress and state. Dieterich¹⁰³ [eq. (A17)] explicitly describes how a stress change perturbs the sliding-speed (and thereby, the time to failure):

$$\frac{\dot{d}}{\dot{d}_0} = \left(\frac{s}{s_0} \right)^{a/A} \exp \left(\frac{t}{As} - \frac{t_0}{As_0} \right), \quad (9)$$

where, \dot{d}_0 , t_0 , and s_0 are the sliding speed, shear stress, and effective normal stress (which includes pore pressure effects) on the nearby fault before the stress change, and \dot{d} , t , and s are the sliding speed, shear stress and effective normal stress (positive for compression) after the stress change. a is a sum of parameters governing normal-stress dependence of the state variables. We note that eqs (8) and (9) are approximations to more complicated forms and assume that the fault is at the stage where slip is accelerating so that the slip speed, \dot{d} , greatly exceeds a steady-state speed, D_c/q (ref. 103).

Harris and Simpson⁵⁴ used the above equations and examined how a rate-and-state 'stress shadow' should appear, and compared it with a CFS-shadow. They applied the shadow calculation to sites in the San Francisco Bay area of California and found that the rate-and-state formulations¹⁰³ are consistent with Bay area seismic history, for a very wide range (several orders of magnitude) of the rate-and-state parameters.

Gomberg *et al.*⁹³ and Gomberg *et al.*¹⁰⁵ have used rate-and-state theory to examine the opposite effect, stress triggering. Gomberg *et al.*⁹³ suggest that earthquakes may be triggered by transient, oscillatory loads (also see Scholz¹⁰² for an opposing viewpoint) or that these loads may trigger earthquakes that would not have occurred without the stress changes generated by another earthquake. That is, some earthquakes were not only clock-advanced by a previous event, but they were also created. Gomberg *et al.*¹⁰⁵ studied the effect of loading history on triggering, both on time scales of the earthquake cycle (tens or hundreds of years) and of seismic waves (seconds to minutes). They also explicitly compared the predictions of the Dieterich rate-and-state frictional model with those of Coulomb shear stress change calculations (assuming constant normal stress).

Dieterich's¹⁰³ equations can also predict aftershock rates. Gross and Kisslinger¹⁰⁶ solved for some variables in the rate-and-state equations (e.g. for A and s) by examining the aftershocks of the 1992 Landers earthquake. Gross and Bürgmann⁸⁷ followed a similar tactic and investigated the aftershocks of the 1989 M 6.9 Loma Prieta earthquake. Toda *et al.*⁶⁰ used Dieterich's¹⁰³ formulations and investigated the aftershock rates of the 1995 Kobe earth-

quake. They used the Kobe aftershock data to determine values for some of the rate-and-state parameters, and also to determine earthquake probabilities based on the stress change calculations.

Dynamic stresses

Far-field (distant) triggering

In addition to static stress changes, dynamic or transient stress changes may be capable of triggering earthquakes. We have evidence from a few large and great earthquakes that distant triggering has occurred. Lomnitz¹⁰⁷ suggested, from the distances where the triggering is observed, that the triggering is due to deep-seated flow in the earth, in a response to the triggering earthquake. Alternatively, dynamic strains may be the cause of some of the distant triggering, but, large regions of the earth's crust are not responding to these strain changes by producing triggered earthquakes. Parkfield, California may be the most famous case of this situation. With Parkfield we have one of the world's more expected (or overdue) earthquakes, and yet it has not been triggered by dynamic strains from recent nearby or distant earthquakes^{108,109}. Spudich *et al.*¹⁰⁹ found that peak dynamic stress of 0.1 MPa (1 bar) after the Landers earthquake did not trigger an expected Parkfield, California earthquake, although distant triggering due to Landers appears to have occurred in other locations¹¹⁰.

A recent earthquake in the Mojave Desert, which occurred 20 to 30 km east of the Landers earthquake may provide more clues about dynamic triggering processes. The 16 October 1999 magnitude 7.1 Hector Mine earthquake produced higher amplitude seismic waves at seismometers to the south of the earthquake than at seismometers to the north of the earthquake, the opposite from the 1992 Landers earthquake which generated higher amplitude waves to the north. There was also significantly more distant triggered seismicity to the south following Hector Mine and to the north following Landers. Therefore, the dynamic waves generated by each of the earthquakes played a role in determining the subsequent patterns of triggered seismicity.

In addition to earthquakes, nature provides a longer period dynamic stressing process with which to study earthquake triggering, the earth's tides. Vidale *et al.*¹¹¹ examined the effects of tidal stresses in earthquake triggering. Through inspection of tidal stresses at the times of > 13,000 earthquakes, Vidale *et al.* found that earthquakes are randomly distributed throughout the tidal cycle. Therefore, dynamic stress rates as large as 10^{-2} MPa/h (10^{-2} bar/h) are not preferentially triggering earthquakes. This is quite significant since tidal stressing rates are much higher than the tectonic loading rates we usually associate with earthquake occurrence. The find-

ings of Vidale *et al.* were corroborated by Lockner and Beeler's¹¹² laboratory experiments. Lockner and Beeler show that only about 1% of earthquakes should correlate with tidal triggering, and that triggering is controlled by both amplitude and frequency of the stresses.

Near-field triggering

The aforementioned studies were for the far-field, where dynamic stress changes greatly exceed static stress changes, but in the near-field, both may be important¹². In the near-field, inter-earthquake dynamic effects (stress waves) may be determining the size of the mainshock itself^{113–118}. This is observed in situations where one earthquake triggers another event within seconds. When this intra-event triggering occurs along fault-strike or even closeby, the result is a much larger earthquake or a multiple event. Examples include the 1992 Landers, California and 1999 Izmit, Turkey earthquakes. The resulting implications for seismic hazard cannot be overstated.

Viscoelastic models

At the other end of the spectrum from dynamic triggering in the near-field, are models that include the effects of long-term loading and relaxation of the lithosphere and asthenosphere. Most of the static stress change models discussed previously are elastic approximations of the earth's crust and upper mantle and do not explicitly include long-term viscoelastic behaviour. A few authors have added a viscoelastic effect, to better model the complete earthquake cycle, or to account for a long time between the initial event(s) and a 'triggered' event¹¹⁹. Dmowska *et al.*¹²⁰ used a 1D model to look at stress fluctuations during the earthquake cycle in coupled subduction zones, to show when and where large after shocks and subsequent mainshocks could occur. Taylor *et al.*¹²¹ used 2D models of earthquake cycles in a generic subduction zone to illustrate the effect of viscoelastic relaxation in both the mantle and shallow portion of the thrust zone on the timing of seismicity in the outer-rise and at intermediate depth. In another tectonic setting, Pollitz and Sacks⁴⁹ used viscoelastic triggering and proposed that the 1995 Kobe, Japan earthquake was 'triggered' by two earthquakes that occurred 50 years before Kobe.

Viscoelastic analyses have also been performed for earthquakes in transform faulting regions. Roth¹⁶ examined the seismicity in the western part of the North Anatolian fault zone, using both elastic and viscoelastic models. He found good agreement between the spatial and temporal pattern of $M \geq 6$ earthquakes, for both types of models. Ben-Zion *et al.*¹²² included viscoelastic loading to show how two great earthquakes on the San Andreas fault, 1857 Ft. Tejon and 1906 San Francisco, California may have modulated the timing of moderate Parkfield, Cali-

fornia, earthquakes. Parkfield is located on a section of the San Andreas fault between the two great ruptures. Ben-Zion *et al.* concluded that the closer 1857 great earthquake, most likely had influenced the timing of moderate Parkfield events, but that 1906 earthquake was too distant to greatly impact the timing. Ghosh *et al.*¹²³ examined the generic 2D case of two parallel strike-slip faults in an elastic layer overlying a viscoelastic halfspace. They showed how creep on one or both of the faults would change the potential of earthquakes on neighbouring faults. The study by Ghosh *et al.* showed an additional time dependence of the shear stresses that is not present in an elastic analysis. Similarly, Kenner and Segall¹²⁴ proposed that the simple elastic models commonly in use do not do justice to the earth's time-dependent material properties. They examined the case of the 1906 San Francisco earthquake and showed how a 2D model that includes a viscoelastic lower crust might perturb the duration and magnitude of a stress-shadow on the Hayward fault from elastic estimates.

There is still a debate about the role of viscoelastic behaviour in the earthquake cycle. Some authors^{125,126} propose that afterslip continues on the fault plane of the earthquake, whereas others^{127,128} propose that a viscoelastic response in the lower crust better explains post-seismic behaviour. Which of these mechanisms is actually in effect has implications for the durations and patterns of the calculated stress changes.

Implications for seismic hazard

Probability estimates

Although many of the calculations performed to date enjoy at least moderate credibility within the scientific community, potential benefits to the public may be lost if the results are not converted into societally useful numbers. In an attempt to remedy this, Cornell *et al.*¹²⁹, Stein *et al.*⁵¹ and Toda *et al.*⁶⁰ have taken their static stress change models for nearby faults and converted the results into earthquake probability estimates. Toda *et al.* performed the calculations for Japan, in the wake of the 1995 Kobe earthquake.

The 17 August 1999 magnitude 7.4 earthquake in Izmit, Turkey, which killed more than 15,000 people¹³⁰, may be the first widely-publicized case where pre-earthquake probability estimates had included stress change calculations. Stein *et al.*⁵¹ incorporated the stressing history of previous known earthquakes on the North Anatolian fault and an assumed deep slip (fault loading) rate into rate-and-state friction formulations. They then estimated the probability of future earthquake occurrence on a number of segments of the North Anatolian fault, including a section near Izmit. Shortly after the August 1999 earthquake, a number of scientists claimed success in forecasting the

Izmit event using stress change calculations, including authors of Stein *et al.*⁵¹ and Nalbant *et al.*⁵⁶.

Following the August Izmit earthquake, a few scientists updated their stress change calculations and presented their preferred locations for a subsequent large earthquake. Although a magnitude 7.1 earthquake did occur on 12 November 1999 at the eastern end of the Izmit rupture, a site anticipated by Barka^{130,131}, most other forecasts have concentrated on a rupture in the Marmara Sea region to the west. This future quake is envisioned to put Turkey's population centre of Istanbul at high risk^{68,130}.

What we have learnt

From our extensive, internationally-distributed set of inter- and intra- earthquake stress change calculations, we have been able to glean some understanding of earthquake behaviour. We have learnt that small, medium, and large aftershocks generally do occur in regions that were 'stressed up' by a mainshock, and that damaging earthquakes generally do not occur in stress-shadowed regions that remain relaxed following the stress change effects of nearby great earthquakes. This latter effect is most obvious in the wake of earthquakes such as the 1906 San Francisco earthquake^{32,42,54}, the 1857 Ft. Tejon earthquake^{38,46}, and the 1891 Nobi earthquake³⁶. All of these great earthquakes shut off subsequent large earthquakes for decades on faults that were relaxed by the great events.

Smith and Van de Lindt⁴ and King *et al.*³⁰ have extended the stress-shadow idea to a role in rupture termination. They argue that the extent of earthquake rupture may be controlled by the static stress effects of previous events. At least in a few cases, it appears that a large earthquake starting in a region of static stress increase may have terminated when it encountered a region of static stress decrease. This may have been what happened for the *M* 6.7 Big Bear, California earthquake³⁰.

The magnitude problem

Ideally stress change calculations could predict where and when to expect large damaging aftershocks. Instead, what the stress change calculations generally provide is just a range of aftershock nucleation sites, but no magnitude information. The models do not *a priori* place a limit on the extent of rupture (magnitude), except as a statistical phenomenon¹⁰³. One type of quasi-static model that does look at the potential maximum magnitude is that of Miller *et al.*¹³². In the Miller *et al.* hypothesis, the effect of a nearby earthquake reducing the normal stress on a fault is to delay a large earthquake from occurring, whereas small earthquakes could still occur. The effect of a nearby earthquake increasing the normal stress is to advance the time to the next large earthquake. This hypothesis does,

however, need more testing to determine whether or not it is applicable to most crustal faults⁵⁴.

The maximum-magnitude question is most likely also a dynamics problem. Once a large aftershock has been nucleated, is its magnitude already pre-determined, do geometrical fault features control the rupture extent, or is the answer in the along-strike and along-dip strength heterogeneity? It is clear that although we have learnt much about earthquake patterns, we are just beginning to scratch the surface when it comes to incorporating earthquake physics into our models.

Future research

The research performed to date still leaves many questions unanswered. Some believe that static stress calculations have predictive power in estimating where future large earthquakes will occur⁶⁷. If that is true, then what can we do with the information that an earthquake-producing fault has received an increase in stress? And, even if the stress increase does generate an immediate crustal response, can we determine if it will be aseismic or seismic? These were some of the questions after the 1992 Landers earthquake and still are questions today.

Stress change calculations may be a valuable tool for evaluating many traits of earthquake occurrence. But do we understand enough about the physics of earthquake nucleation and propagation to translate the simple estimates made by stress change calculations into formal earthquake predictions? The answer for now is 'no'. Perhaps the answer will change in the future as we acquire more information from both past and present earthquakes.

1. Harris, R. A., *J. Geophys. Res.*, 1998, **103**, 24347–24358.
2. McGarr, A. and Simpson, D., in *Rockbursts and Seismicity in Mines* (eds Lasocki, S. and Gibowicz, S.), Balkema, Rotterdam, 1997, pp. 385–396.
3. Simpson, D. W., *Annu. Rev. Earth. Planet. Sci.*, 1986, **14**, 21–42.
4. Smith, S. W. and Van de Lindt, W., *Bull. Seismol. Soc. Am.*, 1969, **59**, 1569–1589.
5. Rybicki, K., *Phys. Earth Planet. Inter.*, 1973, **7**, 409–422.
6. Yamashina, K., *Tectonophysics*, 1978, **51**, 139–154.
7. Yamashina, K., *Phys. Earth Planet. Inter.*, 1979, **18**, 153–164.
8. Das, S. and Scholz, C., *Bull. Seismol. Soc. Am.*, 1981, **71**, 1669–1675.
9. Stein, R. S. and Lisowski, M., *J. Geophys. Res.*, 1983, **88**, 6477–6490.
10. Mavko, G. M., *J. Geophys. Res.*, 1982, **87**, 7807–7816.
11. Mavko, G. M., Schulz, S. and Brown, B. D., *Bull. Seismol. Soc. Am.*, 1985, **75**, 475–489.
12. Rybicki, K., Kato, T. and Kasahara, K., *Bull. Earthquake Res. Inst. Univ. Tokyo*, 1985, **60**, 1–21.
13. Kato, T., Rybicki, K. and Kasahara, K., *Tectonophysics*, 1987, **144**, 181–188.
14. Li, V. C., Seale, S. H. and Cao, T., *Tectonophysics*, 1987, **144**, 37–54.
15. Oppenheimer, D. H., Reasenber, P. A. and Simpson, R. W., *J. Geophys. Res.*, 1988, **93**, 9007–9026.
16. Roth, F., *Tectonophysics*, 1988, **152**, 215–226.

17. Simpson, R. W., Schulz, S. S., Dietz, L. D. and Burford, R. O., *Pure Appl. Geophys.*, 1988, **126**, 665–685.
18. Hudnut, K. W., Seeber, L. and Pacheco, J., *Geophys. Res. Lett.*, 1989, **16**, 199–202.
19. Yoshioka, S. and Hashimoto, M., 1989a, **58**, 173–191.
20. Yoshioka, S. and Hashimoto, M., *Phys. Earth Planet. Inter.*, 1989b, **56**, 349–370.
21. Okada, Y. and Kasahara, K., *Tectonophysics*, 1990, **172**, 351–364.
22. Michael, A. J., *J. Geophys. Res.*, 1991, **96**, 6303–6319.
23. Das, S., *Nature*, 1992, **357**, 150–153.
24. Harris, R. A. and Simpson, R. W., *Nature*, 1992, **360**, 251–254.
25. Jaumé, S. C. and Sykes, L. R., *Science*, 1992, **258**, 1325–1328.
26. Reasenber, P. A. and Simpson, R. W., *Science*, 1992, **255**, 1687–1690.
27. Stein, R. S., King, G. C. P. and Lin, J., *Science*, 1992, **258**, 1328–1332.
28. Du, Y. and Aydin, A., *J. Geophys. Res.*, 1993, **98**, 9947–9962.
29. Oppenheimer, D. H. *et al.*, *Science*, 1993, **261**, 433–438.
30. King, G. C. P., Stein, R. S. and Lin, J., *Bull. Seismol. Soc. Am.*, 1994, **84**, 935–953.
31. Robinson, R., *J. Geophys. Res.*, 1994, **99**, 9663–9679.
32. Simpson, R. W. and Reasenber, P. A., in US Geological Survey Professional Paper 1550-F (ed. Simpson, R. W.), 1994.
33. Stein, R. S., King, G. C. P. and Lin, J., *Science*, 1994, **265**, 1432–1435.
34. Bennett, R. A., Reilinger, R. E., Rodi, W., Li, Y. and Toksöz, M. N., *J. Geophys. Res.*, 1995, **100**, 6443–6461.
35. Harris, R. A., Simpson, R. W. and Reasenber, P. A., *Nature*, 1995, **375**, 221–224.
36. Pollitz, F. F. and Sacks, I. S., *Bull. Seismol. Soc. Am.*, 1995, **85**, 796–807.
37. Deng, J. and Sykes, L. R., *Geophys. Res. Lett.*, 1996, **23**, 1155–1158.
38. Harris, R. A. and Simpson, R. W., *Geophys. Res. Lett.*, 1996, **23**, 229–232.
39. Hodgkinson, K. M., Stein, R. S. and King, G. C. P., *J. Geophys. Res.*, 1996, **101**, 25459–25471.
40. Hubert, A., King, G., Armijo, R., Meyer, B. and Papanastasiou, D., *Earth Planet. Sci. Lett.*, 1996, **142**, 573–585.
41. Jacques, E., King, G. C. P., Tapponnier, P., Ruegg, J. C. and Manighetti, I., *Geophys. Res. Lett.*, 1996, **23**, 2481–2484.
42. Jaumé, S. C. and Sykes, L. R., *J. Geophys. Res.*, 1996, **101**, 765–789.
43. Nalbant, S. S., Barka, A. A. and Alptekin, Ö., *Geophys. Res. Lett.*, 1996, **23**, 1561–1564.
44. Bürgmann, R., Segall, P., Lisowski, M. and Svarc, J., *J. Geophys. Res.*, 1997, **102**, 4933–4955.
45. Caskey, S. J. and Wesnousky, S. G., *Bull. Seismol. Soc. Am.*, 1997, **87**, 521–527.
46. Deng, J. and Sykes, L. R., *J. Geophys. Res.*, 1997a, **102**, 9859–9886.
47. Deng, J. and Sykes, L. R., *J. Geophys. Res.*, 1997b, **102**, 24411–24435.
48. Nostro, C., Cocco, M. and Belardinelli, M. E., *Bull. Seismol. Soc. Am.*, 1997, **87**, 234–248.
49. Pollitz, F. F. and Sacks, I. S., *Bull. Seismol. Soc. Am.*, 1997, **87**, 1–10.
50. Reasenber, P. A. and Simpson, R. W., in US Geological Survey Professional Paper 1550-D (ed. Reasenber, P. A.), 1997, D49–D71.
51. Stein, R. S., Barka, A. A. and Dieterich, J. H., *Geophys. J. Int.*, 1997, **128**, 594–604.
52. Delouis, B., Philip, H., Dorbath, L. and Cisternas, A., *Geophys. J. Int.*, 1998, **132**, 302–338.
53. Hardebeck, J. L., Nazareth, J. J. and Hauksson, E., *J. Geophys. Res.*, 1998, **103**, 24427–24437.
54. Harris, R. A. and Simpson, R. W., *J. Geophys. Res.*, 1998, **103**, 24439–24451.
55. Mikumo, T., Miyatake, T. and Santoyo, M. A., *Bull. Seismol. Soc. Am.*, 1998, **88**, 686–702.
56. Nalbant, S. S., Hubert, A. and King, G. C. P., *J. Geophys. Res.*, 1998, **103**, 24469–24486.
57. Nostro, C., Stein, R. S., Cocco, M., Belardinelli, M. E. and Marzocchi, W., *J. Geophys. Res.*, 1998, **103**, 24487–24504.
58. Singh, S. K., Anderson, J. G. and Rodriguez, M., *Geofis. Int.*, 1998, **37**, 3–15.
59. Taylor, M. A. J., Dmowska, R. and Rice, J. R., *J. Geophys. Res.*, 1998, **103**, 24523–24542.
60. Toda, S., Stein, R. S., Reasenber, P. A., Dieterich, J. H. and Yoshida, A., *J. Geophys. Res.*, 1998, **103**, 24543–24565.
61. Troise, C., De Natale, G., Pingue, F., Petrazzuoli, S. M., *Geophys. J. Int.*, 1998, **134**, 809–817.
62. Fox, C. G. and Dziak, R. P., *J. Geophys. Res.*, 1999, **104**, 17603–17615.
63. Mikumo, T., Singh, S. K. and Santoyo, M. A., *Bull. Seismol. Soc. Am.*, 1999, **89**.
64. Parsons, T., Stein, R. S., Simpson, R. W. and Reasenber, P. A., *J. Geophys. Res.*, 1999, **104**, 20183–20202.
65. Pauchet, H., Rigo, A., Rivera, L., Souriau, A., *Geophys. J. Int.*, 1999, **137**, 107–127.
66. Perfettini, H., Stein, R. S., Simpson, R. W. and Cocco, M., *J. Geophys. Res.*, 1999, **104**, 20169–20182.
67. Stein, R. S., *Nature*, 1999, **402**, 605–609.
68. Hubert-Ferrari, A., Barka, A., Jacques, E., Nalbant, S. S., Meyer, B., Armijo, R., Tapponnier, P. and King, G. C. P., *Nature*, 2000, **404**, 269–273.
69. Chinnery, M. A., *Bull. Seismol. Soc. Am.*, 1963, **53**, 921–932.
70. Weertman, J. and Weertman, J., *Elastic Dislocation Theory*, MacMillan, New York, 1964, pp. 213.
71. Okada, Y., *Bull. Seismol. Soc. Am.*, 1992, **82**, 1018–1040.
72. Shen, Z.-K., Jackson, D. D., Feng, Y., Cline, M., Kim, M., Fang, P. and Bock, Y., *Bull. Seism. Soc. Am.*, 1994, **84**, 780–791.
73. Jaeger, J. C. and Cook, N. G. W. *Fundamentals of Rock Mechanics*, Methuen and Co., London, 1969, pp. 513.
74. Lienkaemper, J. J., Galehouse, J. S. and Simpson, R. W., *Science*, 1997, **276**, 2014–2016.
75. Rice, J. R. and Cleary, M. P., *Rev. Geophys. Space Phys.*, 1976, **14**, 227–241.
76. Roeloffs, E. A., *J. Geophys. Res.*, 1988, **93**, 2107–2124.
77. Roeloffs, E. A., *Adv. Geophys.*, 1996, **37**, 135–195.
78. Skempton, A. W., *Géotechnique*, 1954, **4**, 143–147.
79. Hart, D. J., MS thesis, University of Wisconsin, Madison, 1994, p. 44.
80. Berge, P. A., Wang, H. F. and Bonner, B. P., *Int. J. Rock Mech. Min. Sci. Geomech. Abstr.*, 1993, **30**, 1135–1141.
81. Green, D. H. and Wang, H. F., *Geophysics*, 1986, **51**, 948–956.
82. Wang, H. F., 1997, **102**, 17943–17950.
83. Rice, J. R., in *Fault Mechanics and Transport Properties of Rock: A Festschrift in Honor of W. F. Brace* (eds Evans, B. and Wong, T. -F.), Academic Press, 1992, pp. 475–503.
84. Beeler, N. M., Simpson, R. W., Lockner, D. A. and Hickman, S. H., *J. Geophys. Res.*, 2000 (in press).
85. Kagan, Y. Y., *Geophys. Journ. Int.*, 1994, **117**, 345–364.
86. Kagan, Y. Y. and Jackson, D. D., *J. Geophys. Res.*, 1998, **103**, 24453–24467.
87. Gross, S. and Bürgmann, R., *J. Geophys. Res.*, 1998, **103**, 4915–4927.
88. Nur, A. and Booker, J. R., *Science*, 1972, **175**, 885–887.
89. Noir, J., Jacques, E., Békri, S., Adler, P. M., Tapponnier, P. and King, G. C. P., *Geophys. Res. Lett.*, 1997, **24**, 2335–2338.
90. Mendoza, C. and Hartzell, S. H., *Bull. Seismol. Soc. Am.*, 1988, **78**, 1438–1449.

91. Scholz, C. H., *The Mechanics of Earthquakes and Faulting*, Cambridge University Press, 1990, pp. 439.
92. Anderson, G. and Johnson, H., *J. Geophys. Res.*, 1999, **104**, 20153–20168.
93. Gomberg, J., Blanpied, M. L. and Beeler, N. M., *Bull. Seismol. Soc. Am.*, 1997, **87**, 294–309.
94. Beroza, G. C. and Zoback, M. D., *Science*, 1993, **259**, 210–213.
95. Dodge, D. A., Beroza, G. C. and Ellsworth, W. L., *J. Geophys. Res.*, 1995, **100**, 9865–9880.
96. Dodge, D. A., Beroza, G. C. and Ellsworth, W. L., *J. Geophys. Res.*, 1996, **101**, 22371–22392.
97. Kilb, D., Ellis, M., Gomberg, J. and Davis, S., *Geophys. J. Int.*, 1997, **128**, 557–570.
98. Crider, J. G. and Pollard, D. D., *J. Geophys. Res.*, 1998, **103**, 24373–24391.
99. Axen, G. J., *Geophys. Res. Lett.*, 1999, **26**, 3693–3696.
100. Astiz, L., Shearer, P. M. and Agnew, D. C., *J. Geophys. Res.*, 2000, **105**, 2937–2953.
101. Stuart, W. D. and Tullis, T. E., *J. Geophys. Res.*, 1995, **100**, 24079–24099.
102. Scholz, C. H., *Nature*, 1998, **391**, 37–42.
103. Dieterich, J., *J. Geophys. Res.* 1994, **99**, 2601–2618.
104. Dieterich, J. H. and Kilgore, B., *Proc. Nat. Acad. Sci. USA*, 1996, **93**, 3787–3794.
105. Gomberg, J., Beeler, N., Blanpied, M. and Bodin, P., *J. Geophys. Res.*, 1998, **103**, 24411–24426.
106. Gross, S. and Kisslinger, C., *J. Geophys. Res.*, 1997, **102**, 7603–7612.
107. Lomnitz, C., *Bull. Seismol. Soc. Am.*, 1996, **86**, 293–298.
108. Fletcher, J. B. and Spudich, P., *J. Geophys. Res.*, 1998, **103**, 835–854.
109. Spudich, P., Steck, L. K., Hellweg, M., Fletcher, J. B. and Baker, L., *J. Geophys. Res.*, 1995, **100**, 675–690.
110. Hill, D. P. *et al.*, *Science*, 1993, **260**, 1617–1623.
111. Vidale, J., Agnew, D., Johnston, M. and Oppenheimer, D., *J. Geophys. Res.*, 1998, **103**, 24567–24572.
112. Lockner, D. A. and Beeler, N. M., *J. Geophys. Res.*, 1999, **104**, 20133–20151.
113. Harris, R. A., Archuleta, R. J. and Day, S. M., *Geophys. Res. Lett.*, 1991, **18**, 893–896.
114. Harris, R. A. and Day, S. M., *J. Geophys. Res.*, 1993, **98**, 4461–4472.
115. Harris, R. A. and Day, S. M., *Geophys. Res. Lett.*, 1999, **26**, 2089–2092.
116. Kase, Y. and Kuge, K., *Geophys. J. Int.*, 1998, **135**, 911–922.
117. Belardinelli, M. E., Cocco, M., Coutant, O. and Cotton, F., *J. Geophys. Res.*, 1999, **104**, 14925–14946.
118. Magistrale, H. and Day, S., *Geophys. Res. Lett.*, 1999, **26**, 2093–2096.
119. Freed, A. M. and Lin, J., *J. Geophys. Res.*, 1998, **103**, 24393–24409.
120. Dmowska, R., Rice, J. R., Lovison, L. C. and Josell, D., *J. Geophys. Res.*, 1988, **93**, 7869–7884.
121. Taylor, M. A. J., Zheng, G., Rice, J. R., Stuart, W. D. and Dmowska, R., *J. Geophys. Res.*, 1996, **101**, 8363–8381.
122. Ben-Zion, Y., Rice, J. R. and Dmowska, R., *J. Geophys. Res.*, 1993, **98**, 2135–2144.
123. Ghosh, U., Mukhopadhyay, A. and Sen, S., *Phys. Earth Planet. Inter.*, 1992, **70**, 119–129.
124. Kenner, S. and Segall, P., *Geology*, 1999, **27**, 119–122.
125. Bock, Y., Wdowinski, S., Fang, P., Zhang, J., Williams, S., Johnson, H., Behr, J., Genrich, J., Dean, J., *J. Geophys. Res.*, 1997, **102**, 18013–18033.
126. Donnellan, A. and Lyzenga, G. A., *J. Geophys. Res.*, 1998, **103**, 21285–21298.
127. Deng, J., Gurnis, M., Kanamori, H. and Hauksson, E., *Science*, 1998, **282**, 1689–1692.
128. Deng, J., Hudnut, K., Gurnis, M., Hauksson, E., *Geophys. Res. Lett.*, 1999, **26**, 3209–3212.
129. Cornell, C. A., Wu, S. –C., Winterstein, S. R., Dieterich, J. H. and Simpson, R. W., *Bull. Seismol. Soc. Am.*, 1993, **83**, 436–449.
130. Barka, A., *Science*, 1999, **285**, 1858–1859.
131. Barka, A., *Bull. Seismol. Soc. Am.*, 1996, **86**, 1238–1254.
132. Miller, S. A., Nur, A. and Olgaard, D. L., *Geophys. Res. Lett.*, 1996, **23**, 197–200.

ACKNOWLEDGEMENTS. Versions of this manuscript benefited from the helpful reviews of Nick Beeler, Massimo Cocco, Renata Dmowska, Joan Gomberg, Hiroo Kanamori, Art McGarr, Kusala Rajendran, Bob Simpson, David Simpson, Bill Stuart and Lynn Sykes. Thanks to Kusala Rajendran for inviting my participation in this special section.